Romanian Journal of Petroleum & Gas Technology
Vol. VII (LXXVIII) • No. 1/2026

INTEGRATED INTERPRETATION OF THE L59 PROFILE IN THE CENTRAL BASIN (DRC): STRUCTURAL ANALYSIS, SEISMOSTRATIGRAPHY, AND PETROPHYSICAL MODELING OF RESERVOIRS

Joel Etshekodi Lohadje [1,2*], Franck Tondozi Keto [3,4], Marlin Agolo Monza [2]

[1] Geological Survey, D.R. Congo
[2] Faculty of Petroleum, Gas, and Renewable Energy, University of Kinshasa, D.R. Congo
[3] Faculty of Science and Technology, University of Kinshasa, D.R. Congo
[4] Geophysical Research Center, D.R. Congo
* Email (corresponding author): joellohadje@gmail.com

DOI: 10.51865/JPGT.2026.01.11

ABSTRACT

This study takes us to the heart of the Central Basin of the Democratic Republic of Congo, a sedimentary giant still shrouded in geological mystery. To uncover its oil potential, we carefully examined seismic profile L59. Over 180 km, cross-analysis of key attributes such as envelope, RMS amplitude, and sweetness enabled us to redraw the subsurface architecture.

We identified six major sedimentary sequences that tell the story of the basin: an alternation of promising sandstone reservoirs and clay layers acting as natural caps. The discovery of "bright spots" is particularly encouraging, as these anomalies often indicate the presence of hydrocarbons trapped by the movements of salt and crystalline bedrock.

To transform these acoustic images into concrete data, we used Wyllie's formula to estimate a porosity of approximately 13.4% at the Gilson well. Based on Tarantola's theories (2005), we then extrapolated these properties to the entire reservoir using an exponential decay model. This approach led us to an initial estimate of the original oil in place (OOIP). Although these calculations are based on mathematical models, they confirm that the L59 profile area is a prime target for future exploration drilling.

Keywords: Central Basin, seismostratigraphy, seismic attributes, petrophysical modeling, petroleum potential

INTRODUCTION

The Central Basin of the Democratic Republic of Congo is one of the largest sedimentary basins on the African continent. However, despite its enormous size, it remains largely unknown in terms of its geology, stratigraphy, and petroleum resources. Although seismic data exists and a few exploration wells, such as Samba and Gilson, have been drilled, our understanding of the deep architecture of the basin and the structures favorable to hydrocarbon trapping remains unclear. This lack of clarity is mainly due to the limited number of wells available, some of which have not even reached the crystalline basement, making stratigraphic correlations particularly complex.

This is where detailed analysis of existing seismic profiles comes into its own. The L59 profile, which stretches for approximately 180 km, offers an exceptional window into the tectonic structures and stratigraphy of this region. However, a simple visual reading is not enough to unravel the complexity of the subsurface; it has become essential to use advanced modeling tools and seismic attributes to obtain an accurate picture of the geological reality.

The objective of this study is therefore to shed light on the oil potential of the sector crossed by line L59. By analyzing the seismostratigraphic organization and modeling key parameters such as porosity and water saturation, we are laying the necessary groundwork for a serious assessment of the area's resources.

MATERIALS AND METHODS

The methodological approach of this study is based on an integrated approach combining geophysical processing, seismostratigraphic interpretation, and petrophysical modeling. The core of our analysis is based on the use of seismic profile L59, which was processed and interpreted using state-of-the-art PETREL and GOCAD software. These tools enabled multidimensional analysis (2D and 3D), which is essential for transforming raw acoustic signals into a coherent geological image. In order to refine the detection of subtle structures and potential reservoirs, we calculated several seismic attributes. By accentuating acoustic impedance contrasts and lateral discontinuities, these attributes facilitated the identification of seismostratigraphic sequences and the understanding of sedimentary body geometry [1].

In parallel with seismic imaging, quantitative characterization of the reservoirs was carried out. Geometric modeling of the formations was based on converting seismic times into actual depths using root mean square (VRMS) propagation velocities. This crucial step enabled accurate estimation of the thickness and lateral extent of the identified structures. For the petrophysical dimension, essential parameters such as porosity and water saturation were calculated from log data obtained from reference wells in the Central Basin. Finally, to compensate for the scarcity of direct control points, these petrophysical data were spatially extrapolated using horizontal and vertical variation models, in accordance with Tarantola's parameter estimation principles [2]. The final integration of this information, as well as the production of thematic maps (isobaths, isopachs, and iso-properties), was carried out using SURFER software. This rigorous methodological framework thus ensures the transition between geophysical observation and quantitative assessment of the petroleum potential of the studied area.

RESULTS

This study consists of the processing and stratigraphic and structural interpretation of seismic profile L59, followed by the log interpretation of the Gilson and Mbandaka wells to deduce porosity and saturation for modeling purposes. These elements will enable us to estimate the volume of hydrocarbons in place.

Taken along the road over a distance of 180 km, the profile of line L59, visualized using GOCAD reservoir modeling software, shows the seismic signatures illustrated in Figure 1. This seismic profile was used for the Dekese drilling project, which aimed to determine the lithostratigraphy of the Central Basin. Unfortunately, this drilling did not reach the bedrock and no logging was performed.

Romanian Journal of Petroleum & Gas Technology
Vol. VII (LXXVIII) • No. 1/2026

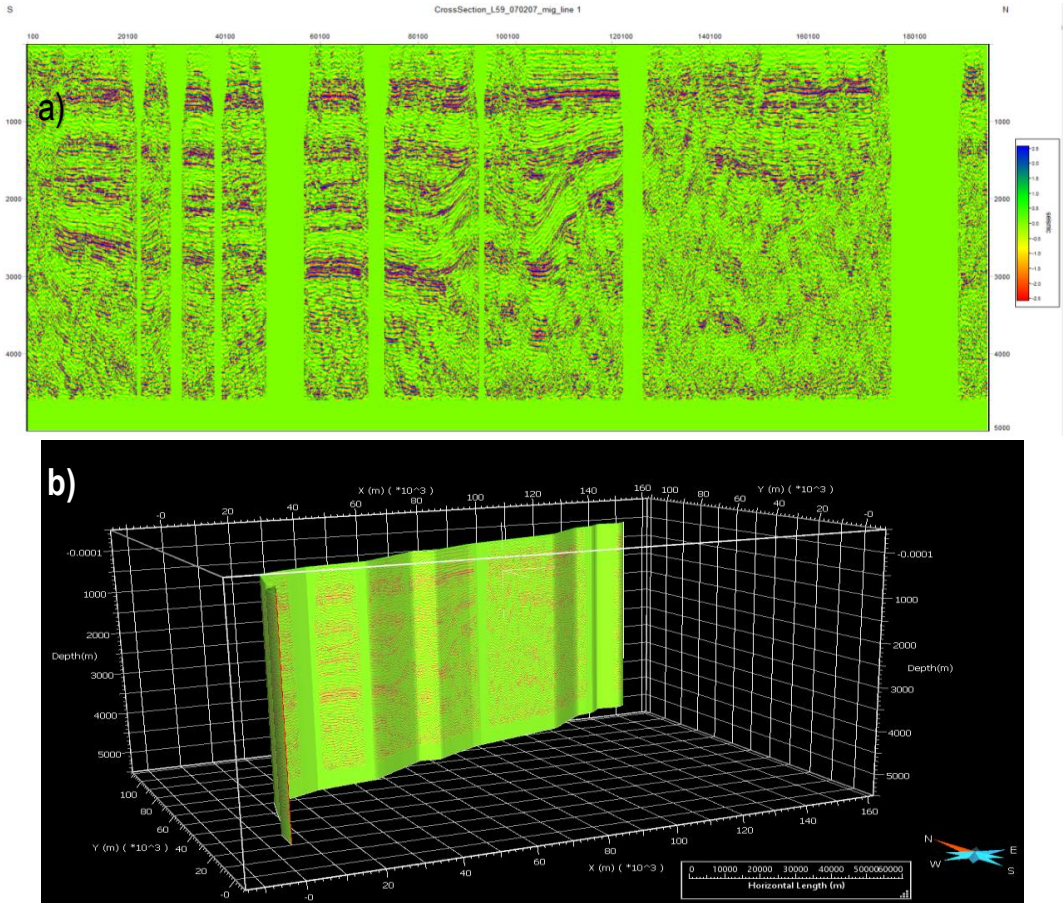

Figure 1. *Seismic section L59 (a) 2D model, and b) 3D model).*

Processing and interpretation of seismic profile L59

A. Envelope attribute

The envelope attribute or reflection intensity displays acoustically strong (bright) events over negative and positive events. It is the most popular trace attribute. It is calculated from the complex trace of the seismic signal used to highlight the main seismic characteristics [3],[4].

The envelope represents the instantaneous energy of the signal, and its magnitude is proportional to the reflection coefficient [5]. The envelope is useful for highlighting discontinuities, lithology changes, faults, deposit variation, tuning effects, and sequence boundaries [6]. The bright spots in this attribute are important because they can indicate gas, especially in relatively young clastic sediments [7]. The advantage of using this attribute instead of the original seismic trace values is that it is independent of the phase or polarity of the seismic data, which affects the apparent brightness of a reflection [8]. Bright spots probably correspond to channel bodies or sand layers due to acoustic impedance contrast. Faults in the envelope attribute are typically characterized by lateral discontinuities.

However, it is difficult to observe the seismic attribute [9]. The study of the seismic envelope attribute on the profiles selected in our study area indicates a variation in acoustic impedance contrast related to the difference in rock formation densities and wave velocity [10]. This contrast provides information on lithological changes on the one hand and sequence boundaries

Romanian Journal of Petroleum & Gas Technology
Vol. VII (LXXVIII) • No. 1/2026

on the other [11]. The bright spots represent sequences rich in coarse grains, which in this case are mainly sandstone, while the light blue color on these seismic lines represents low-energy sequences that mainly contain very fine grains, shales. The "sapphire blue" color indicates carbonate sequences [12].

In seismic profile L59, we identified six sequences (Figure 2) that can be described as follows:

- The S1 sequence, which is mainly clayey with a significant carbonate component, lies on the bedrock and could correspond to the Ituri clay-limestone formation.
- Sequence S2 is mainly sandstone, tabular, and is thought to correspond to the Bokwamboli sandstone formation. It would be a good reservoir rock.
- Sequence S3 is mainly clayey with carbonate interbeds. Referring to the stratigraphic scale of the Central Basin, it would correspond to the Mamungi Shale.
- Sequence S4 is thought to be Galambodge sandstone, in which we find a significant portion of carbonate.
- Sequence S5 is deposited in discordance (Pan-African discordance) on the bedrock in the SW and sequence S4 (Galambodge sandstone) in the NE. This sequence could correspond to the Alolo Shale.
- Sequence S6 consists of carbonate, shown here by a low acoustic impedance contrast and bright spots indicating the presence of coarse-grained rocks. The formation is thought to be the Lukuga sandy carbonate.

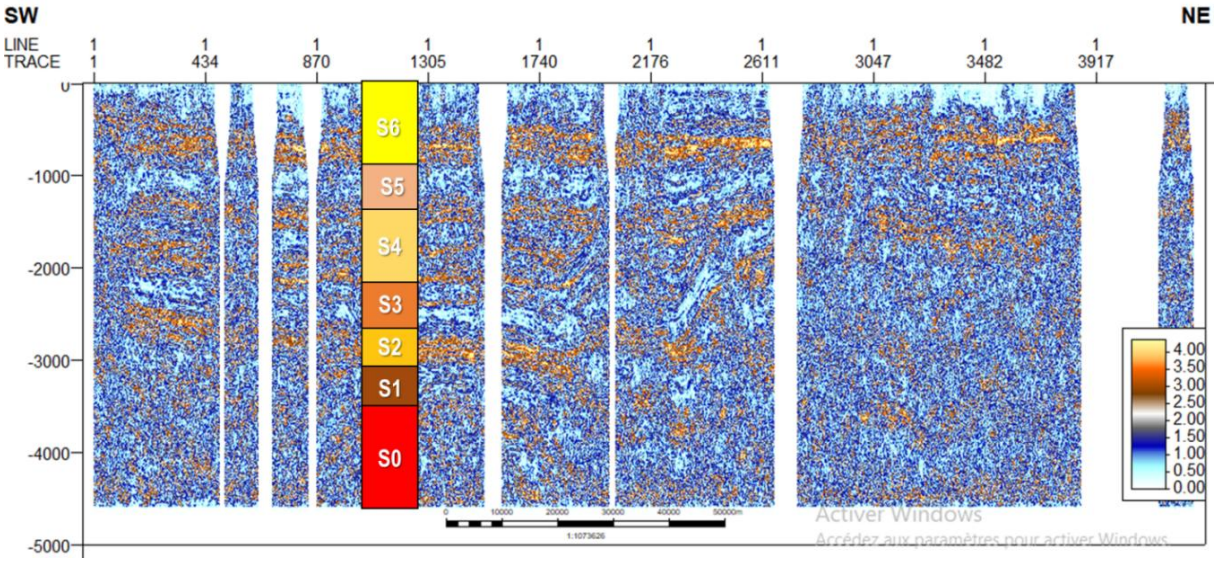

Figure 2. *Stratigraphic interpretation of seismic profile L59.*

B. Root Mean Square (RMS) Amplitude

The root mean square (RMS) amplitude provides a scaled estimate of the trace envelope. It is calculated in a tapered sliding window of N samples as the square root of the sum of all trace values squared, where w and n are the window values [13],[14].

RMS amplitude is similar to a smoother version of reflection strength. It is applied in the same way as reflection strength to reveal bright spots and amplitude anomalies in seismic data [1]. Unlike reflection strength, the resolution can be adjusted by changing the window length.

Romanian Journal of Petroleum & Gas Technology
Vol. VII (LXXVIII) • No. 1/2026

Longer windows produce a smoother estimate of amplitude, which is sometimes useful. This attribute is useful for highlighting coarser-grained facies, compaction effects [e.g., in marls and limestones), and unconformities [7].

The interpretation of the mean square amplitude attribute (Figure 3) is as follows:

- Sequence 6 consists of coarse and fine grains.
- Sequence 5 consists of fine grains.
- Sequence 4 consists of alternating coarse and fine grains. This sequence forms a multi-layer reservoir. It consists of alternating porous and permeable layers with impermeable layers that serve as caps.
- Sequence 3, consisting of fine grains that can serve as source rocks or caps.
- Sequence 2: may correspond to a reservoir rock, as we observe a high intensity of reflections that may indicate the presence of coarse grains and empty spaces containing fluids (gas, oil, and water).
- Sequence 1: produces weak reflections, which allows us to classify it as source rock.
- Sequence 0: consists solely of metamorphic bedrock.

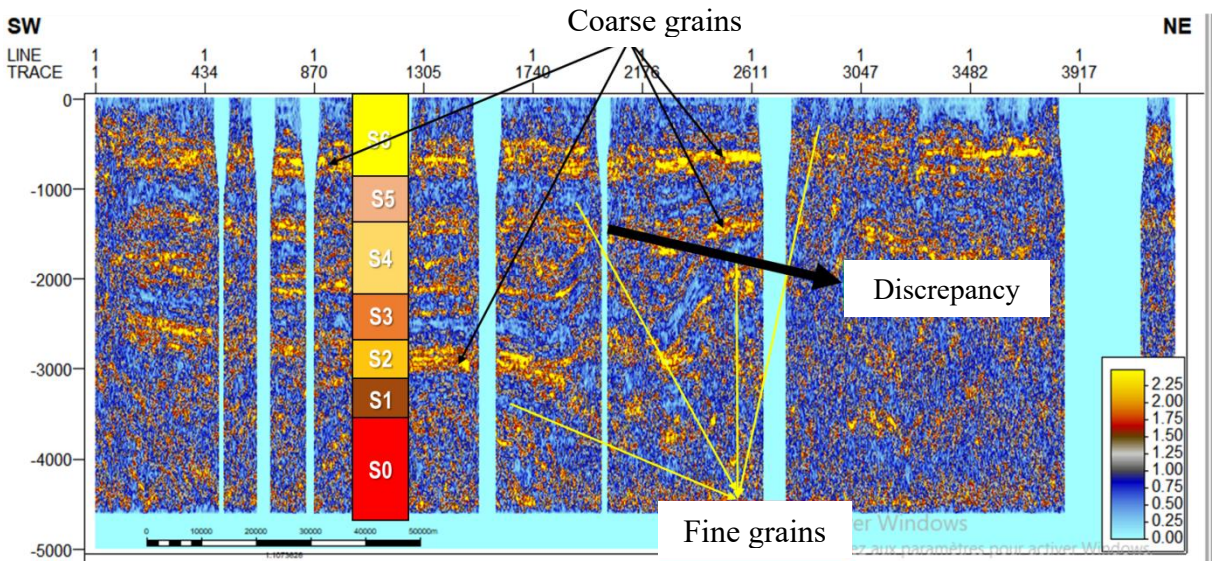

Figure 3. *Root Mean Square Amplitude of Seismic Profile L59.*

C. Sweetness of Seismic Profile L59

Sweetness (instantaneous amplitude divided by the square root of the instantaneous frequency) is defined as the envelope of trace *a(t)* divided by the square root of the average frequency *fa(t)* [3]. Sweetness is an attribute designed to identify "sensitive areas," areas prone to oil and gas, and improves the imaging of relatively coarse-grained (sand) intervals or bodies [14]. The definition of smoothness is motivated by the observation that, in young clastic sedimentary basins, sensitive areas identified on seismic data generally have high amplitudes and low frequencies. Therefore, high smoothness values are those most likely to indicate oil and gas [15]. Smoothness anomalies of interest therefore correspond to reflection strength anomalies.

Romanian Journal of Petroleum & Gas Technology
Vol. VII (LXXVIII) • No. 1/2026

Hart [31] suggests that smoothness is particularly useful for channel detection. Anomalies in this attribute are sometimes located in a similar location to amplitude and RMS envelope attributes due to their physical properties. Furthermore, it has been shown that the smoothness attribute of the plan view shows geomorphic features such as sand bodies of point bars and distribution channels in great detail [16].

Geophysicists look for positive amplitude anomalies that may indicate the presence of hydrocarbons [13]. An increase in amplitude may suggest an accumulation of gas or oil, while a decrease could indicate the presence of water or other unwanted fluids [10]. Calculating the Sweetness attribute will enable us to highlight the probable presence of hydrocarbons within potential structures that constitute hydrocarbon traps.

The study of the L59 seismic profile revealed the presence of several characteristic seismic anomalies: “bright spots”. These anomalies appear as particularly reflective areas on seismic recordings. In petroleum geophysics, bright spots are often interpreted as potential indicators of the presence of hydrocarbons [15]. The bright spots identified on the L59 profile suggest the possibility of hydrocarbon accumulations within the underlying geological structures. The presence of fluids such as oil or gas within rocks can alter their physical properties and thus generate these characteristic seismic anomalies.

A total of eight areas of interest have been identified on the L59 seismic profile (Figure 4), each with bright spots. These areas are located within geological structures considered to be hydrocarbon traps, i.e., geological structures capable of capturing and retaining hydrocarbons. Detailed geological analysis has determined the origin of these geological structures. They result from the combination of two major tectonic processes: salt tectonics and the influence of the crystalline basement [17],[18]. These processes have created conditions favorable to the formation of geological traps and the accumulation of hydrocarbons. The presence of multiple bright spots associated with complex geological structures makes the L59 profile a particularly promising exploration area. Additional studies, such as geochemical analyses and exploratory drilling, will be necessary to confirm the presence of commercially viable hydrocarbons in these areas.

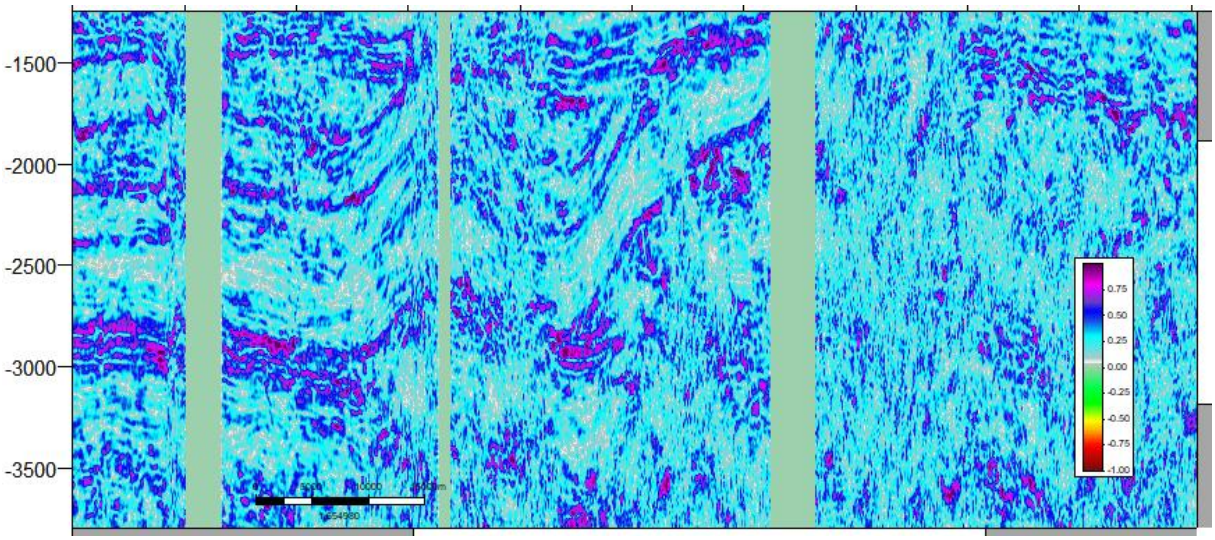

Figure 4. *Sweetness of seismic profile L59.*

Romanian Journal of Petroleum & Gas Technology
Vol. VII (LXXVIII) • No. 1/2026

D. Reflection intensity

The reflection intensity (or reflection amplitude) attribute is used to analyze acoustic impedance contrasts in seismic data. This attribute helps identify geophysical anomalies that are often associated with changes in lithology, reservoir fluids, or porosity [10],[14],[17]. Reflection intensity is a key indicator in hydrocarbon detection because it reveals amplitude anomalies, such as bright spots and dim spots, which may indicate the presence of gas or oil [20].

Reflection intensity is directly related to the variation in acoustic impedance between two geological layers. When hydrocarbons are present in a reservoir, they modify this acoustic impedance, which results in an amplitude anomaly on the seismic signal [15],[21].

This attribute is used in the following main applications:

- Hydrocarbon detection (bright spot, dim spot, flat spot),
- Reservoir characterization (porous zones, fluid saturation),
- Identification of fluid contacts (gas-water, oil-water),
- Mapping of faults and fractures (structural traps).

When a reservoir contains hydrocarbons, the reduction in density and acoustic velocity in pores saturated with gas or oil causes an amplitude anomaly on the seismic profile. This anomaly can be interpreted as a direct indicator of the presence of hydrocarbons [7].

For example:

- A bright spot (high positive amplitude) may indicate a gas-saturated reservoir.
- A dim spot (reduced amplitude) may indicate the transition from a water-saturated zone to a hydrocarbon-saturated zone.

We have identified four areas of interest that may contain hydrocarbons (Figure 5). These bright spot and dim spot areas are located between 1,500 and 3,000 mS double time. The stratigraphic and structural model of this seismic profile L59 is shown in Figure 6. Identification of the hydrocarbon zone in the central part of seismic profile L59 considering all seismic attributes: envelope, sweetness, and mean square amplitude is shown in Figure 7.

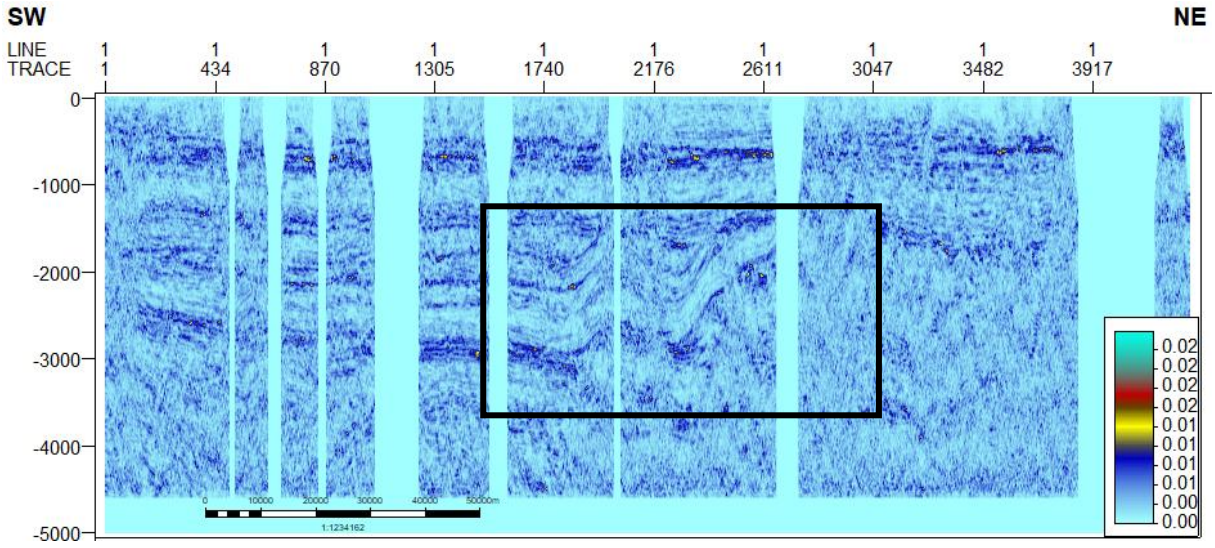

Romanian Journal of Petroleum & Gas Technology
Vol. VII (LXXVIII) • No. 1/2026

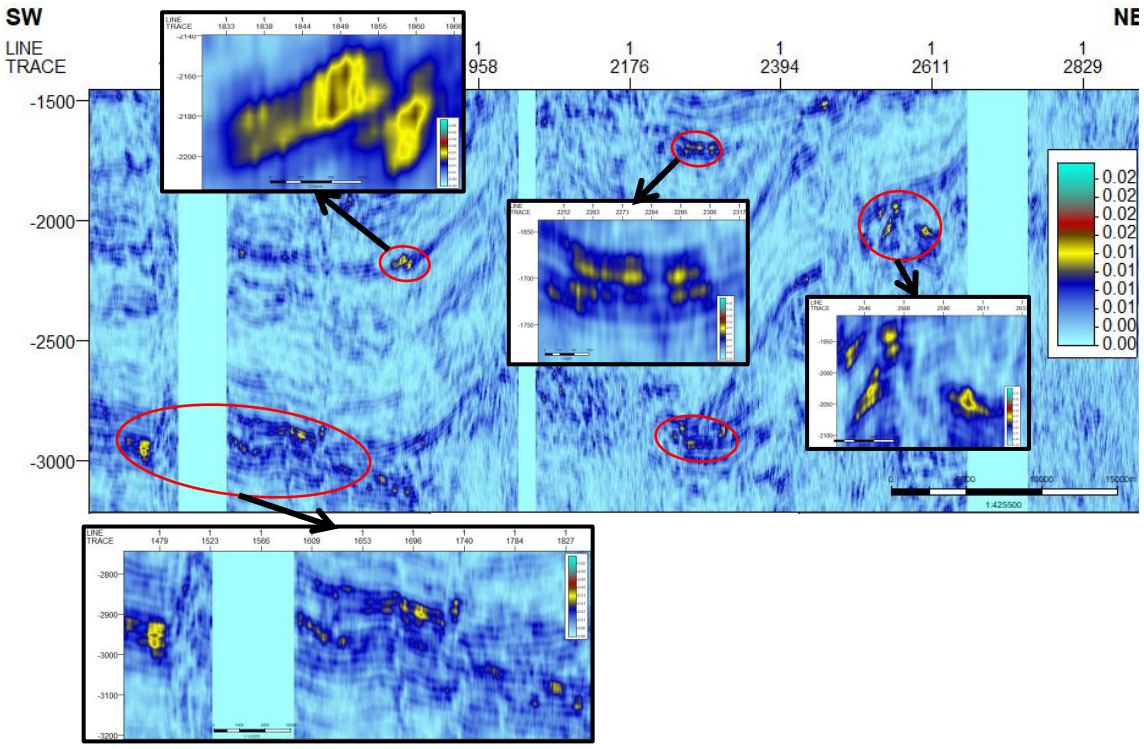

Figure 5. *Identification of hydrocarbon zones based on reflection intensity in profile L59.*

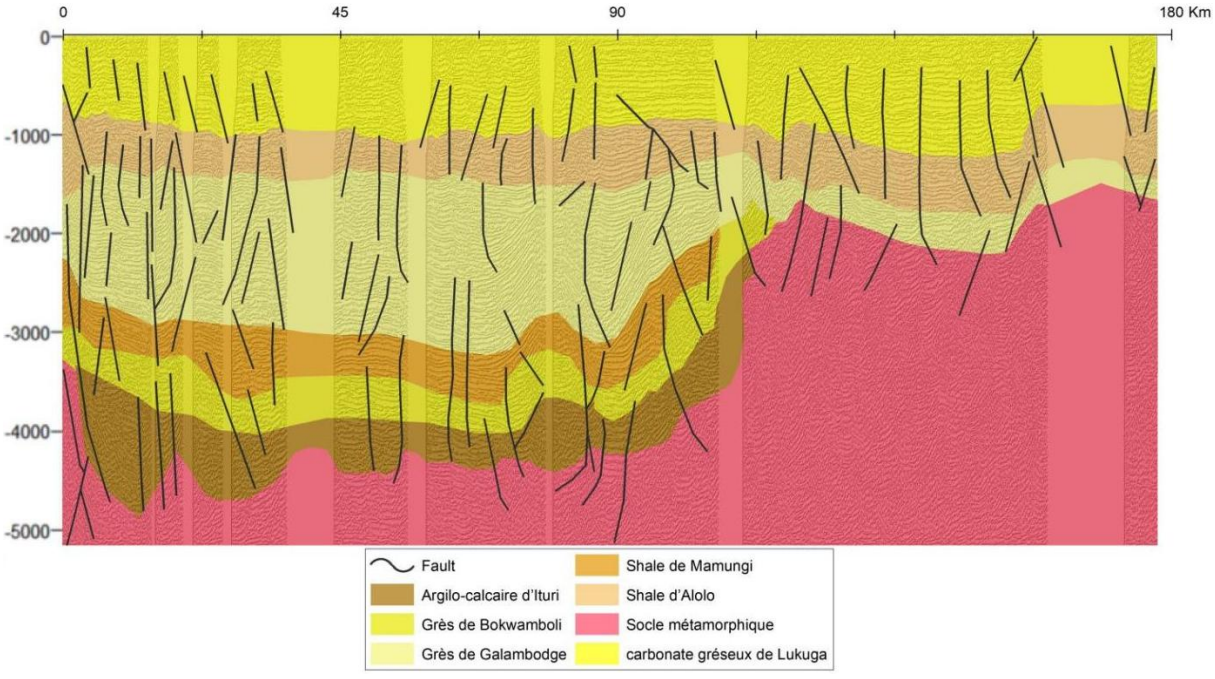

Figure 6. *Stratigraphic and structural interpretation in seismic profile L59.*

Romanian Journal of Petroleum & Gas Technology
Vol. VII (LXXVIII) • No. 1/2026

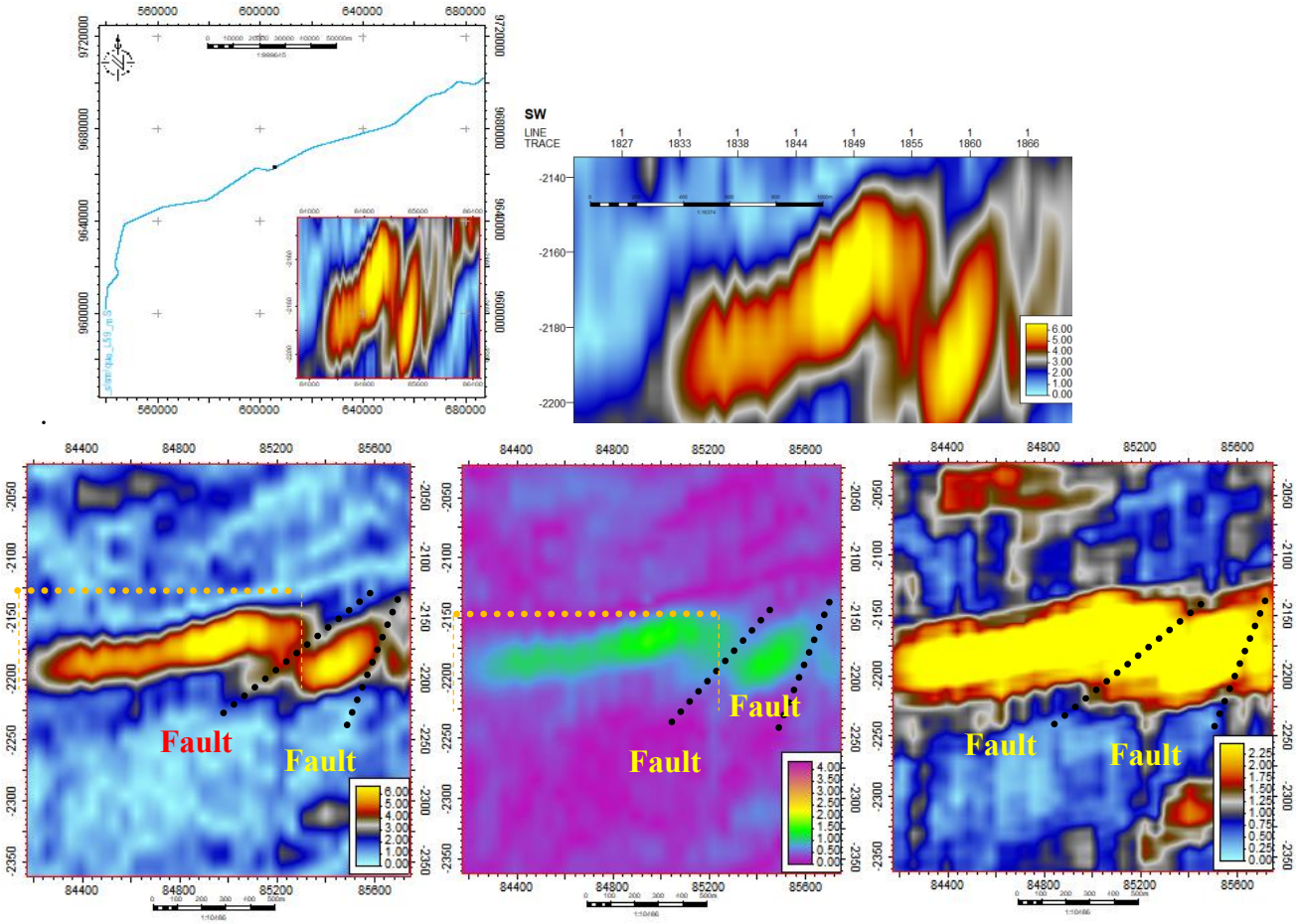

Figure 7. *Identification of the hydrocarbon zone in the central part of seismic profile L59. a) envelope attribute; b) sweetness; c) mean square amplitude attribute.*

E. Calculation of hydrocarbon reserves in the Lokoro sub-basin

Applying the volumetric method, the oil volume in place is calculated by the following formula [22],[23]:

$$N = \frac{S*H_u*\emptyset_m*(1-S_{wm})}{B_{oi}} \quad (1)$$

- N: oil reserves in place (m3);
- S: area surface;
- Hu: useful height;
- Boi: initial volumetric oil factor;
- $\emptyset_m$: porosity;
- S_{wm}: irreducible water saturation.

After measuring the depths of the roof and walls of reservoir 1, we will need to know the lateral extension to the right and left to model the reservoir geometrically. To do this, we will apply simplified geometric modeling (Figure 8) with axial symmetry to determine the geometry or dimensions (length, width, and depth of the roof and walls) in 2D and 3D of this reservoir 1.

Romanian Journal of Petroleum & Gas Technology
Vol. VII (LXXVIII) • No. 1/2026

According to the principle of axial symmetry, the total width of a symmetrical structure is evenly distributed on either side of the axis of symmetry, with each side having a lateral extension equal to half the total width.

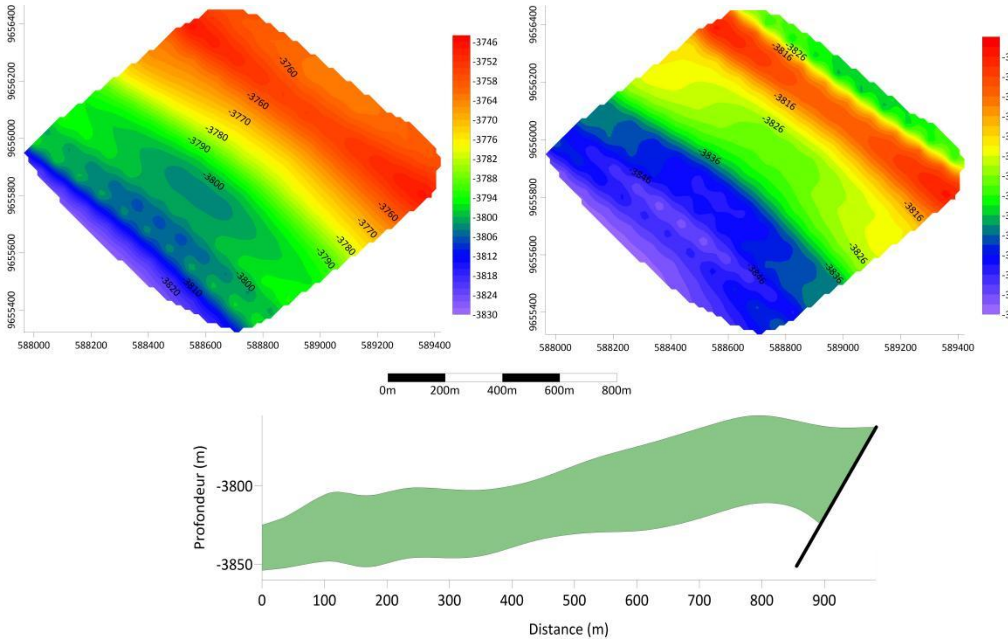

Figure 8. *a) isobath of the reservoir wall; b) isobath of the reservoir roof; c) structural model of the reservoir (fault).*

– Calculation of thickness in meters

The equation used to calculate the depth in meters to the roof and walls, knowing the double round trip time and the root mean square velocity in this reservoir rock, which is equal to 3300 m/s [24], is as follows:

$$h_{toit} = \frac{V*T}{2} \quad (2)$$

$$\left.\begin{array}{l} h_{toit} = \frac{V*T_{toit}}{2} \\ h_{Murs} = \frac{V*T_{Murs}}{2} \end{array}\right\}$$

$$h\_roof\_wall\ (m) = \left(\frac{\frac{3300}{1000} * \quad}{2} \right) \quad (3)$$

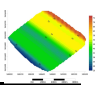

The thickness will be the difference between the depth at the walls and at the roof of reservoir_1.

$$E_{Murs} = h_{roof\ (m)} - h_{walls\ (m)} \quad (4)$$

The map of isobaths in the reservoir 1 is shown in Figure 9.

Romanian Journal of Petroleum & Gas Technology
Vol. VII (LXXVIII) • No. 1/2026

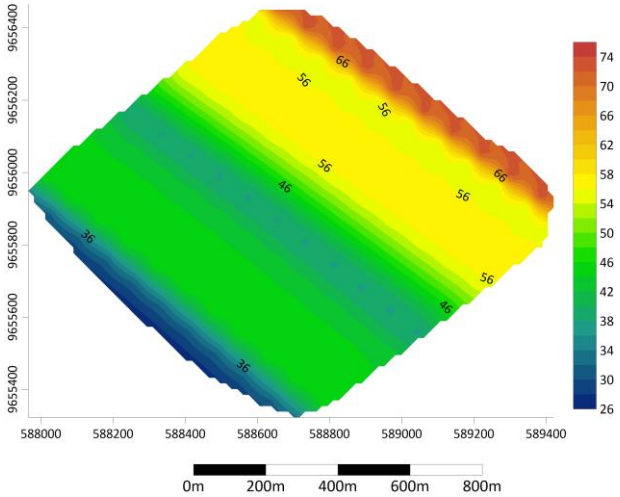

Figure 9. *Map of isobaths in reservoir 1.*

– **Modeling petrophysical parameters (porosity and water saturation)**

When only a single porosity value is available at a specific point, extrapolating this value over a given surface represented by a mesh (or grid) is very difficult. It requires making strong assumptions about how porosity might vary in space. Knowing the porosity and saturation values that we can read on the sonic and resistivity logs of the wells drilled in the Central Basin, we can model the assumptions used to extrapolate from the known values.

In fact, [2] in his book "Problem Theory and Methods for Model Parameter Estimation", defines three assumptions for determining petrophysical properties (porosity and water saturation) extrapolating in the reservoir. Since the entire model is not cited, we considered the exponential decay model, which is written as follows:

$$\emptyset_{(x,y)} = \emptyset_{Gilson} * e^{\alpha d} * e^{-\beta h} \quad (5)$$

- Ø(x,y): Porosity at a given point.
- Ø(Gilson): Porosity in the Gilson borehole or reference porosity.
- β: Vertical decay coefficient.
- α: Horizontal decay coefficient.

– **Determination of Porosity**

Porosity can be estimated from sonic log data using Wyllie's equation, also known as the mean time formula. This method is based on the transit time of acoustic waves through a formation, which is related to porosity and material properties.

– **Wyllie Formula**

The Wyllie formula for calculating porosity is given by [25],[26]:

$$\emptyset = \frac{\Delta t_{log} - \Delta t_{matrix}}{\Delta t_{fluid} - \Delta t_{matrix}} \quad (6)$$

Although this study is based on porosities derived from acoustic logs, the transformation of these measurements using Wyllie's law requires cautious interpretation. The sonic device quantifies a transit time, which it converts into porosity based on an assumed uniform matrix velocity. However, this approach can mask the physical complexity of the subsurface,

particularly in the presence of heterogeneous lithologies or microfracture networks. It is therefore essential to combine these results with a sensitivity study of the V_{ma} and V_f variables in order to accurately reflect the petrophysical characteristics of the reservoir.

– **At the Gilson drilling level:**

Δt_{log} = 75 µs/ft (read from sonic log)

The sonic value of the matrix is specific to the lithology of the formation traversed. As the reservoir is of the shale-limestone type, the value of Δt_{matrix} is 55 µs/ft (sandstone). The sonic value of the fluid in the rock pores depends on the nature of the fluid. The fluid to be considered in the calculation of sonic porosity is water with a value of 189 µs/ft (varies according to density and composition).

We can therefore substitute this into the formula to find the porosity:

$$\emptyset_{0\ Gilson} = \frac{75 - 55}{189 - 55} = 0{,}14925373 = 15\ \%$$

– **At the Mbandaka drilling site**

Δt_{log} = 67 µs/ft (read from sonic log at a depth of 12,950 feet or 3,947.16 m)

Δt_{matrix} = 55 µs/ft (clean Bombwambolie sandstone)

Δt_{water} = 189 µs/ft

$$\emptyset_{0\_Mbandaka} = \frac{67 - 55}{189 - 55} = 0{,}08955224 = 9\ \%$$

– **Calculation of the decreasing coefficient**

$$\emptyset(Z) = \emptyset_0 . e^{-\alpha d} \quad (7)$$

$$\emptyset(Z) = \emptyset_0 . e^{-\beta Z} \quad (8)$$

- α: horizontal coefficient; β: vertical coefficient.

We can therefore calculate the distance using the following formula:

$$d_1 = \sqrt{(x_{Mbandaka} - x_{Gilson})^2 + (y_{Mbandaka} - y_{Gilson})^2} \quad (9)$$

- $X_{Mbandaka}$ = 185668,577 m
- $Y_{Mbandaka}$ = 9993493,705 m
- X_{Gilson} = 397615,525 m
- Y_{Gilson} = 9680 940,328 m

– **α: horizontal coefficient**

$$\emptyset_{Mbandaka} = \emptyset_{Gilson} * e^{-\alpha d(x,y)} \quad (10)$$

$$\alpha_{horizontal} = -\frac{\ln\left(\frac{\emptyset_{Mbandaka}}{\emptyset_{Gilson}}\right)}{d_{F(Mbandaka/Gilson)}} \quad (11)$$

$$d_{F(Mbandaka/Gilson)} = \sqrt{(185668{,}577 - 397615{,}525)^2 + (9993493{,}705 - 9680940{,}328)^2}$$

$$d_{F(Mbandaka/Gilson)} = \sqrt{44920816867 + 97659842513} = 377080.56\ m$$

$$\alpha_{horizontal} = -\frac{\ln\left(\frac{0{,}09}{0{,}15}\right)}{377080{,}56} = -0.000000135469\ m^{-1}$$

Romanian Journal of Petroleum & Gas Technology
Vol. VII (LXXVIII) • No. 1/2026

– **β: vertical coefficient**

$$\emptyset_{Mbandaka} = \emptyset_{Gilson} * e^{-\alpha_{vertical}(h_{Mbandaka} - h_{Gilson})} \quad (12)$$

$$\alpha_{vertical} = -\frac{\ln\left(\frac{\emptyset_{Mbandaka}}{\emptyset_{Gilson}}\right)}{(h_{Mbandaka} - h_{Gilson})} \quad (13)$$

$$\alpha_{vertical} = -\frac{\ln\left(\frac{0,09}{0,15}\right)}{(3947,16 - 3878,58)} = -0.007448609\ m^{-1}$$

– **Porosity modeling**

$$\emptyset_{(x,y)} = \emptyset_{Gilson} * e^{-(0,000000135469 * d_{(x,y)} + 0,007448609 * h_{(wall,\ roof)})} \quad (14)$$

The depth we will consider will be the average of the depths of the roof and walls of the reservoir:

$$h_{roof/wall} = \left(\frac{(h_{wall} + h_{roof})}{2} - h_{réf(F.\ Gilson)}\right) \quad (15)$$

$$\begin{cases} \emptyset_1 = 0,15 * e^{-(0,000000135469 * 212134,1786 + 0,007448609 * (-41,9730712))} \\ \emptyset_2 = 0,15 * e^{-(0,000000135469 * 212047,0661 + 0,007448609 * (-41,9730712))} \\ \emptyset_3 = 0,15 * e^{-(0,000000135469 * 211959,9649 + 0,007448609 * 3726,991302)} \\ \emptyset_{4,5,6,7,\ldots,142} = 0,15 * e^{-(0,000000135469 * d_{(4,5,6,7,\ldots,142)} + 0,007448609 * h_{mur/toit\,(4,5,6,7,\ldots,142)})} \\ \emptyset_{143} = 0,15 * e^{-(0,000000135469 * 212220,8877 + 0,007448609 * (-41,97130687))} \end{cases}$$

After calculation, we obtain the following results:

$$\begin{cases} \emptyset_1 = 0,199243072 \\ \emptyset_2 = 0,199245423 \\ \emptyset_3 = 0,199247774 \\ \emptyset_{4,5,6,7,\ldots,142} = 0,15 * e^{-(0,000000135469 * d_{(4,5,6,7,\ldots,142)} + 0,007448609 * h_{mur/toit\,(4,5,6,7,\ldots,142)})} \\ \emptyset_{143} = 0,199240731 \end{cases}$$

The data presented above can be used to produce the iso-porosity map shown in Figure 10. This reveals that, in general, the porosity of the reservoir gradually decreases in a southwesterly direction.

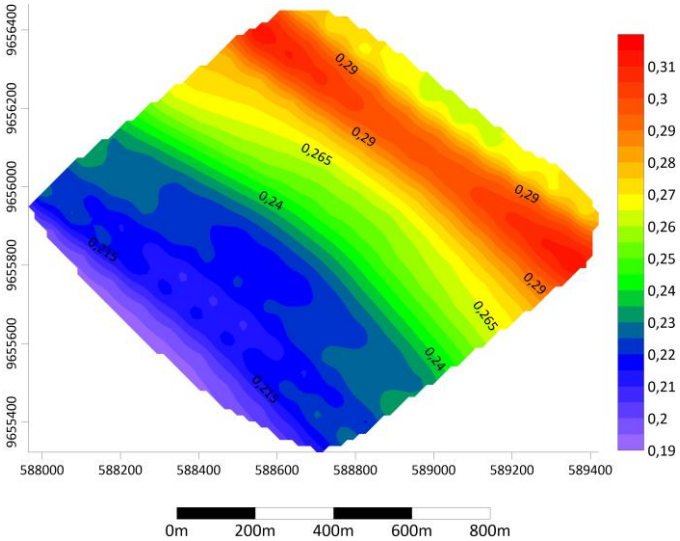

Figure 10. *Map of the spatial distribution of porosity.*

Romanian Journal of Petroleum & Gas Technology
Vol. VII (LXXVIII) • No. 1/2026

– **Saturation calculation**

In the absence of formation tests and despite the dry nature of the well, water saturation was estimated from the graphical logs, assuming that the drilled reservoir intervals are saturated with water. The true formation resistivity *Rt* was read from the deep resistivity logs in clean sandstone levels, then the formation water resistivity *Rw* was deduced by inversion of Archie's law under the assumption *Sw*=1. This *Rw* value was then used to calculate the water saturation in the areas of interest [27].

$$S_w = \sqrt[n]{\frac{F*R_w}{R_t}} \tag{16}$$

$$F = \frac{a}{(\emptyset)^m} \tag{17}$$

$$S_w = \sqrt{\frac{44{,}44*0{,}045}{10}} = 0{,}44719123$$

$$S_{w\_Gilson} = 45\ \%$$

– *Rt* = 0,5 ohm.m

$$R_{w\_Mbandaka} = \frac{0{,}5}{(0{,}09)^{-2}} = 0{,}00405 \text{ ohm.m}$$

$$F = \frac{1}{(0{,}09)^2} = 123{,}45679$$

$$S_{wMbandaka} = \sqrt{\frac{123{,}45679*0{,}00405}{2}} = 0{,}5$$

$$S_{wMbandaka} = 50\%$$

Calculation of the decreasing coefficient

– α: horizontal coefficient

$$\hat{S}_{w(x,y)} = S_{w\,0} * e^{-\alpha d(x,y)} \tag{18}$$

$$\hat{S}_{wMbandaka} = S_{w\,Gilson} * e^{-\alpha d(x,y)} \tag{19}$$

$$0{,}50 = 0{,}45 \,.\, e^{-377080{,}56\alpha_{horizontal}}$$

$$-377080{,}56\ \alpha_{horizontal} = \ln\left(\frac{0{,}50}{0{,}45}\right)$$

$$\alpha_{horizontal} = -0{,}000000279411\ m^{-1}$$

– β: vertical coefficient

$$Sw_{Mbandaka} = Sw_{Gilson} * e^{-\alpha_{vertical}(h_{Mbandaka} - h_{Gilson})} \tag{20}$$

$$\alpha_{vertical} = -\frac{\ln\left(\frac{Sw_{Mbandaka}}{Sw_{Gilson}}\right)}{(h_{Mbandaka} - h_{Ref.\ Gilson})} \tag{21}$$

$$\alpha_{vertical} = -\frac{\ln\left(\frac{0{,}50}{0{,}45}\right)}{(3947{,}16 - 3878{,}58)} = -0{,}001536315\ m^{-1}$$

Romanian Journal of Petroleum & Gas Technology
Vol. VII (LXXVIII) • No. 1/2026

The equation for water saturation thus becomes:

$$Sw_{(x,y)} = Sw_{gilson} * e^{-(0,000000279411 * d_{(x,y)} + 0,001536315 * h_{(mur,\ toit)})} \quad (22)$$

$$h_{mur/toit} = \left(\frac{(h_{toit} + h_{mur})}{2} - h_{réf(F.\ Gilson)}\right) \quad (23)$$

$$\begin{cases} Sw_1 = 0,45 * e^{-(0,000000279411 * 212134,1786 + 0,001536315 * (-41,9730712))} \\ Sw_2 = 0,45 * e^{-(0,000000279411 * 212047,0661 + 0,001536315 * (-41,9730712))} \\ Sw_3 = 0,45 * e^{-(0,000000279411 * 211959,9649 + 0,001536315 * (-41,9730712))} \\ Sw_{(4,5,6,7,.....,142)} = 0,45 * e^{-(0,000000279411 * d_{((4,5,6,7,.....,142))} + 0,001536315 * h_{(mur,\ toit)(4,5,6,7,.....,142)})} \\ Sw_{143} = 0,45 * e^{-(0,000000279411 * 212220,8877 + 0,001536315 * (-41,97130687))} \end{cases}$$

After calculation, we obtain the following results:

$$\begin{cases} Sw_1 = 0,452349951 \\ Sw_2 = 0,452360962 \\ Sw_3 = 0,452371971 \\ Sw_{(4,5,6,7,.....,142)} = 0,45 * e^{-(0,000000279411 * d_{((4,5,6,7,.....,142))} + 0,001536315 * h_{(mur,\ toit)(4,5,6,7,.....,142)})} \\ Sw_{143} = 0,452338992 \end{cases}$$

The results regarding water saturation were used to create a map of water saturation contour lines, to identify areas of the reservoir with high or low saturation values. As shown in Figure 11, the saturation levels increase gradually from the southeast to the northwest.

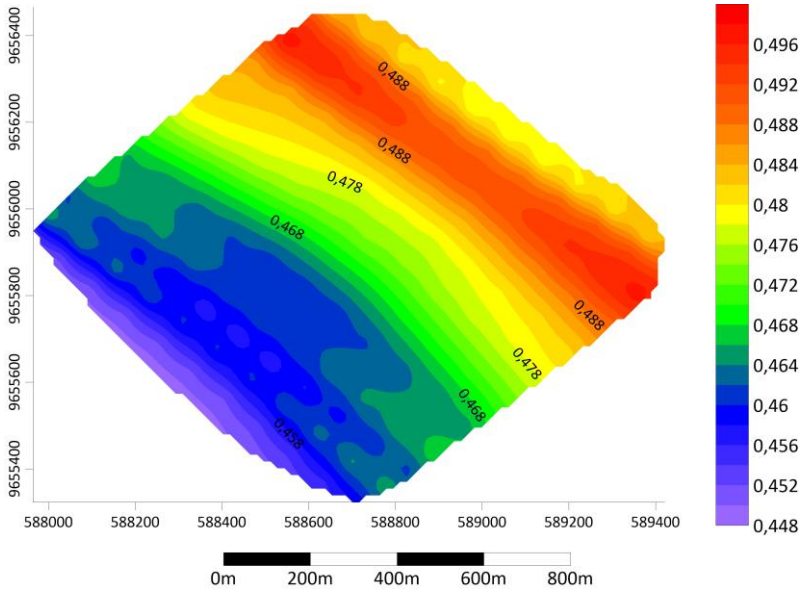

Figure 11. *Map of iso-saturations.*

– Original oil in place (OOIP)

After determination of all parameters, applying the volumetric method was calculated the volume of Original Oil in Place (OOIP) with the formula (1) given previously. In Figure 12 are shown the volumes of hydrocarbon calculated under bottom conditions in the studied area.

Romanian Journal of Petroleum & Gas Technology
Vol. VII (LXXVIII) • No. 1/2026

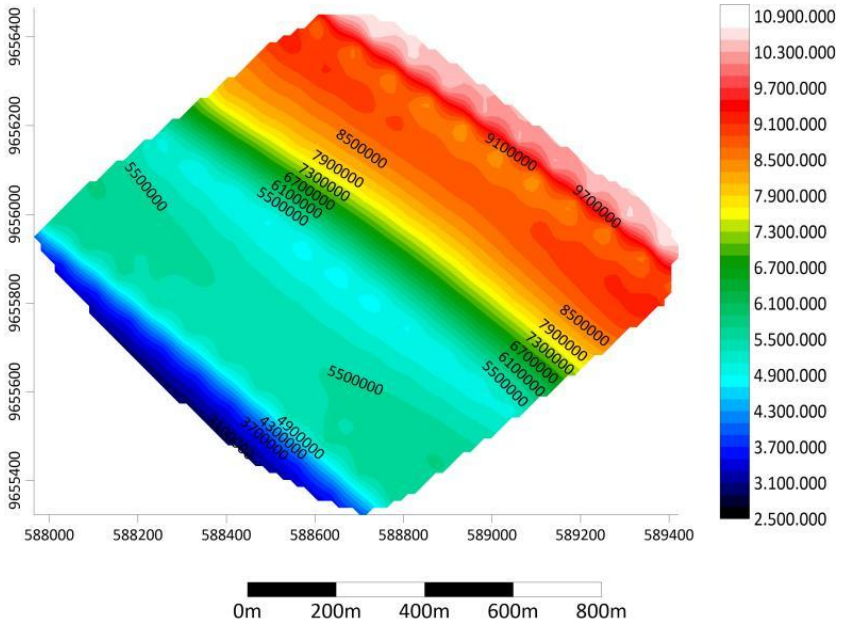

Figure 12. *Hydrocarbon volume under bottom conditions.*

It should be noted that mapping spatial variation allows preferential accumulation zones (sweet spots) to be identified, and is supplemented here by a confidence interval analysis. Extrapolation between wells in a basin as large as Lokoro involves uncertainties inherent in seismic resolution and the assumptions of the Wyllie equation. Thus, the calculated volumes (Figure 12) are accompanied by a range of probabilities between 2 500 000 and 10 900 000 m^3, ensuring that the spatial representation remains consistent with the actual density of the available data.

CONCLUSIONS

Analysis of seismic profile L59 has provided a better understanding of the geological and stratigraphic organization of the Central Basin along a major 180 km axis. By integrating seismic data into GOCAD software and combining several seismic attributes (envelope, RMS, sweetness, and reflection intensity), this study identified six major sedimentary sequences characterized by clear lithological contrasts. These sequences reflect an alternation of fine and coarse rocks, including sandstone and carbonate levels likely to act as reservoirs, as well as clay levels that could constitute source rocks or caps.

In terms of structure and petroleum, the L59 profile reveals a complex geological context, dominated by the combined influence of salt tectonics and the crystalline basement. This configuration has favored the formation of structural traps in which several “Bright Spots” and “Dim Spots” seismic anomalies have been identified. These anomalies, observed at different time depths, are strong indicators of the potential presence of hydrocarbons. Their distribution and association with favorable structures make profile L59 a particularly promising exploration area within the Central Basin.

REFERENCES

[1] Taner, M.T., Seismic Attributes. CSEG Recorder, 26(9), 48-56, 2001.

[2] Tarantola, A., Inverse Problem Theory and Methods for Model Parameter Estimation. Society for Industrial and Applied Mathematics (SIAM), 2005.

[3] Taner, M.T., et al., Seismic attributes revisited. SEG Technical Program Expanded Abstracts, 1994.

[4] Robertson, J.D., Nogami, H.H., Complex seismic trace analysis of thin beds. Geophysics, 49(4), 1984.

[5] Taner, M.T., Koehler, F., Sheriff, R.E., Complex seismic trace analysis. Geophysics, 44(6), 1979.

[6] Chopra, S., Marfurt, K.J., Seismic attributes – A historical perspective. Geophysics, Vol. 70, No. 5, 2005.

[7] Brown, A.R., Interpretation of Three-Dimensional Seismic Data. AAPG Memoir 42, 2011.

[8] Sheriff, R.E., Geldart, L.P., Exploration Seismology. Cambridge University Press, 1995.

[9] Koson, B., et al., Interpretation of Seismic Attributes in Depicting Channel Features and Reservoir Properties. International Journal of Geosciences, 2014.

[10] Veeken, P.C., Seismic Stratigraphy, Basin Analysis and Reservoir Characterization. Elsevier Science. 2007.

[11] Mitchum, R.M., Vail, P.R., Thompson, S., Seismic Stratigraphy and Global Changes of Sea Level. AAPG Memoir. 1977.

[12] Rider, M.H., Bolonne, C., The Geological Interpretation of Well Logs. Rider-French Consulting Ltd. 2011.

[13] Sheriff, R.E., Encyclopedic Dictionary of Applied Geophysics. Society of Exploration Geophysicists. 2002.

[14] Chopra, S., Marfurt, K.J., Seismic Attributes for Prospect Identification and Reservoir Characterization. Society of Exploration Geophysicists [SEG). 2007.

[15] Hilterman, F.J., Seismic Amplitude Interpretation. Distinguished Instructor Series, SEG. 2001.

[16] Koson, B., et al., Application of seismic attributes in fluvial geometry identification. Geosciences Journal. 2014.

[17] Daly, M.C., et al., Tectonic evolution of the Cuvette Centrale, Zaire. Journal of the Geological Society. 1992.

[18] Kadima, E., et al., Structure and geological history of the Congo Basin: An integrated interpretation of gravity, magnetic and reflection seismic data. Journal of African Earth Sciences. 2011.

[19] Sukmono, S., Seismic Attributes for Reservoir Characterization. Departement of Geophysical Engineering, Institut Teknologi Bandung (ITB), Indonésie. 2010.

[20] Taner, M.T., Sheriff, R.E., Application of Amplitude, Frequency, and Other Attributes to Stratigraphic and Hydrocarbon Determination. In: C.E. Payton (Ed.), Seismic Stratigraphy - Applications to Hydrocarbon Exploration, AAPG Memoir 26, pp. 301-327. 1977.

[21] Sheriff, R.E., Geldart, L.P., Exploration Seismology (2nd Edition). Cambridge University Press. 1995.

[22] Dake, L.P., Fundamentals of Reservoir Engineering. Elsevier Scientific Publishing Company. 1978.

[23] Ahmed, T., Reservoir Engineering Handbook. Gulf Professional Publishing. (Excellent pour le détail des paramètres PVT comme le Boi). 2010.

[24] Oil Search / Pioneer International Development, Technical Report on Seismic Interpretation and Velocity Analysis - Congo Basin. 2007.

[25] Wyllie, M.R.J., Gregory, A.R., Gardner, L.W., Elastic wave velocities in heterogeneous and porous media. Geophysics, 21(1), 41-70. (L'article original posant les bases de la formule). 1956.

[26] Wyllie, M.R.J., Gregory, A.R., Gardner, G.H.F., An experimental investigation of factors affecting elastic wave velocities in porous media. Geophysics, 23(3), 459-493. (Étude complémentaire sur les facteurs d'influence). 1958.

[27] Archie, G.E., The Electrical Resistivity Log as an Aid in Determining Some Reservoir Characteristics. Transactions of the AIME, 146(01), 54-62. 1942.

[28] Hart, B.S., Channel detection in 3D seismic data using sweetness: AAPG Bulletin, v.92, 733-742, 2008.

Received: February 2026; Revised: March 2026; Accepted: March 2026; Published: March 2026